JOURNAL OF GUIDANCE, CONTROL, AND DYNAMICS
Vol. 26, No. 2, March–April 2003

Formation Flying: Accommodating Nonlinearity and Eccentricity Perturbations

Sesha S. Vaddi,* Srinivas R. Vadali,† and Kyle T. Alfriend‡
Texas A&M University, College Station, Texas 77843-3141

Hill–Clohessy–Wiltshire equations describe the relative motion of one satellite with respect to another in a circular reference orbit. Initial conditions that generate periodic solutions to these equations have to be corrected to obtain bounded solutions in the presence of nonlinearity of the differential gravitational acceleration model and eccentricity of the reference orbit. The corrections to the initial conditions due to quadratic terms in the differential gravitational acceleration for circular reference orbits are established first by using a perturbation approach. These corrections are related to the period-matching constraint required for bounded relative motion. Next, the solution to the linear problem including the effect of eccentricity is determined, and a procedure for correcting the along-track bias is presented. The two solutions obtained are combined to produce an asymptotic solution for the quadratic eccentricity problem. The effects of nonlinearity and eccentricity on the relative orbits are characterized as functions of their initial position in the formation.

Introduction

THE problem of relative motion dynamics of satellites has been of interest since the 1960s. Much of the work has been performed in the context of the rendezvous problem. Accurate modeling of the relative motion dynamics for initial conditions close to the target is important for the rendezvous problem. Formation flying requires bounded relative motion. Therefore, the solutions of interest are restricted to a certain set of initial conditions that lead to bounded relative motion. One particular formation of interest is the relative orbit that is circular when projected on the local horizontal plane. This solution is an exact solution to Hill–Clohessy–Wiltshire (HCW) equations that model the relative motion dynamics under the assumption of a circular reference orbit, spherical Earth, and linearized differential gravitational acceleration. Nonlinearity of the differential gravitational acceleration, eccentricity of the reference orbit, and the Earth's oblateness are the three most important perturbations that breakdown the circular orbit solutions to HCW equations. In this paper, we study the effects of nonlinearity and the eccentricity perturbations; the effects of J_2 are ignored.

The developments in this paper draw on several previous studies. Melton[1] developed a state transition matrix solution for the linearized relative motion dynamics by incorporating the effect of eccentricity. Inalhan et al.[2] obtained the condition for bounded relative orbit solutions to the linearized problem with nonzero eccentricity. The effects of including quadratic gravitational acceleration terms were studied in Refs. 3–6. Karlgaard and Lutze[7] used the method of multiple timescales to obtain a perturbation solution to the quadratic problem formulated using spherical coordinates. Alfriend et al.[8] used a geometric approach to map relative motion coordinates to orbital element differences. Mitchell and Richardson[9] developed an active nonlinear controller to accommodate quadratic nonlinearities in the zero-eccentricity problem. Broucke[10] has presented an exact state transition matrix solution for the linearized elliptic rendezvous problem. The solution is obtained by taking partial derivatives with respect to orbital elements and requires Kepler's equation to be solved. Yamanaka and Ankersen[11] have also developed a state transition matrix solution for the relative motion on an elliptic orbit by linearizing the governing differential equations. They directly solve the differential equations by taking true anomaly as the independent variable and using a transformation on the relative motion variables.

In this paper, we first review various models of relative motion dynamics. Nonlinearity and eccentricity are identified as the perturbations that breakdown the desired HCW solutions. The effects of these perturbations are first studied independently. Accordingly, in the next section we present a bounded perturbation solution to the problem with nonlinearity and without eccentricity. The perturbation solution is used to generate a correction to the HCW initial conditions. This correction is also related to a period-matching requirement for bounded relative motion between two satellites. Next, we study the linear dynamic model in the presence of eccentricity of the reference orbit. Conditions for bounded solutions developed in Ref. 2 are used to generate another correction to HCW initial conditions. Melton's[1] state transition matrix solution is utilized to obtain a time-explicit representation to the bounded solutions of the linearized relative motion problem with eccentricity. A solution to the same problem is also available in Ref. 2 but as a function of true anomaly rather than time. Melton's[1] state transition matrix involves a series expansion in powers of the eccentricity. Hence, its accuracy is determined by the order of the highest power retained in the series solution. Melton's solution, derived until second order, has been extended to third order. The solution obtained has been further tailored to represent bounded relative orbits. This process leads to another correction to the HCW initial conditions. The two corrections obtained independently are finally combined to produce bounded relative orbit solutions to the nonlinear problem with nonzero eccentricity.

Relative Motion Dynamics

The relative motion dynamics for an eccentric reference orbit is modeled by the following set of nonlinear differential equations:

$$\ddot{x} - 2\dot{\theta}\dot{y} - \ddot{\theta}y - \dot{\theta}^2 x = -\frac{\mu(r_c + x)}{\left[(r_c + x)^2 + y^2 + z^2\right]^{\frac{3}{2}}} + \frac{\mu}{r_c^2}$$

$$\ddot{y} + 2\dot{\theta}\dot{x} + \ddot{\theta}x - \dot{\theta}^2 y = -\frac{\mu y}{\left[(r_c + x)^2 + y^2 + z^2\right]^{\frac{3}{2}}}$$

$$\ddot{z} = -\frac{\mu z}{\left[(r_c + x)^2 + y^2 + z^2\right]^{\frac{3}{2}}}$$

$$\ddot{r}_c = r_c\dot{\theta}^2 - \frac{\mu}{r_c^2}, \qquad \ddot{\theta} = -\frac{2\dot{r}_c\dot{\theta}}{r_c} \tag{1}$$

Received 12 February 2002; revision received 15 August 2002; accepted for publication 12 November 2002.

*Graduate Student, Department of Aerospace Engineering, H.R. Bright Building, Room 611B, Mail Stop 3141 TAMU; vsv8003@aero.tamu.edu.

†Professor, Department of Aerospace Engineering, H.R. Bright Building, Room 727B, Mail Stop 3141 TAMU; svadali@aero.tamu.edu.

‡Wisenbaker II Professor, Department of Aerospace Engineering, H.R. Bright Building, Room 745, Mail Stop 3141 TAMU; alfriend@aero.tamu.edu.

where x, y, and z are the relative motion coordinates of the deputy with respect to the chief in the local-vertical–local-horizontal (LVLH) coordinate system, r_c refers to the scalar radius of the chief from the center of the Earth, θ refers to the latitude angle of the chief, and μ is the graviatational parameter.

The system of equations just presented involves 10 states, and the full-fledged effects of both nonlinearity and eccentricity are accounted for. The effects of eccentricity of the reference orbit that influences the relative motion dynamics of the deputy are captured by the augmented fourth-order dynamics of the chief. This model is referred to as the true model, and the simulations conducted using this model are referred to as the complete nonlinear simulations.

The HCW equations of relative motion for a circular reference orbit are

$$\ddot{x} - 2n\dot{y} - 3n^2x = 0, \qquad \ddot{y} + 2n\dot{x} = 0, \qquad \ddot{z} + n^2z = 0 \quad (2)$$

where $n = \sqrt{(\mu/a_c^3)}$ and a_c is the semimajor axis of the chief.

Note that Eqs. (2) are based upon two approximations: 1) linearization of the differential gravitational acceleration and 2) circular reference orbit assumption. Also note that Eqs. (1) are closer to reality but that Eqs. (2) are the most amenable to analysis.

HCW equations admit a special family of solutions known as the circular projection relative orbits given by

$$x_0 = (\rho/2)\sin(nt + \alpha_0), \qquad y_0 = \rho\cos(nt + \alpha_0)$$
$$z_0 = \rho\sin(nt + \alpha_0) \quad (3)$$

where ρ determines the size of the relative orbit and α_0 is a phase angle. Each deputy in a formation is given a unique α_0. The preceding solution results in a circular relative orbit when projected on to the y–z plane, hence the name projected circular orbit. Shown in Fig. 1 is a snapshot of the formation when the chief is at perigee. The chief is at the center of the relative orbit and the deputies are populated in a circular pattern around it.

There exists another circular orbit solution of the form

$$x_0 = (\rho/2)\sin(nt + \alpha_0), \qquad y_0 = \rho\cos(nt + \alpha_0)$$
$$z_0 = \left(\sqrt{3}\rho/2\right)\sin(nt + \alpha_0) \quad (4)$$

resulting in $x_0^2 + y_0^2 + z_0^2 = \rho^2 = \text{const}$. This solution will be referred to as the general circular orbit.

The two families of solutions to Eqs. (2) are of particular interest to formation flying. In this paper, we only deal with the projected circular orbit, though the ideas are not specific to this orbit alone.

A model that includes quadratic terms in the differential gravity field expansion is shown next. This model, in terms of accuracy, lies between the true model and the linear model

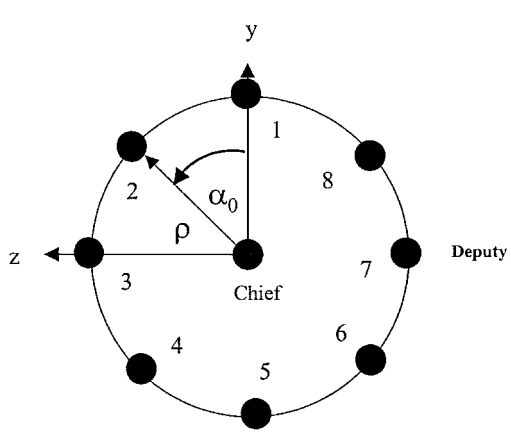

Fig. 1 Snapshot of formation at the perigee of the chief.

(HCW equations):

$$\ddot{x} - 2\dot{\theta}\dot{y} - \ddot{\theta}y - \dot{\theta}^2x - 2\mu x/r_c^3 = \left(3\mu/r_c^4\right)[y^2/2 + z^2/2 - x^2]$$
$$\ddot{y} + 2\dot{\theta}\dot{x} + \ddot{\theta}x - \dot{\theta}^2y + \mu y/r_c^3 = \left(3\mu/r_c^4\right)xy$$
$$\ddot{z} + \mu z/r_c^3 = \left(3\mu/r_c^4\right)xz$$
$$\ddot{r}_c = r_c\dot{\theta}^2 - \mu/r_c^2, \qquad \theta = -(2\dot{r}_c\dot{\theta}/r_c) \quad (5)$$

The analytical results presented are based on the preceding model, but the solutions are evaluated on the true model.

Our objective in this paper is to study the effects of nonlinearity and eccentricity perturbations on the HCW equations and determine approximate solutions to the complete nonlinear problem that are close to the circular orbit solutions. A primary requirement for such solution is that it be bounded. Exciting those solutions that are bounded and close to the circular orbit solutions will be beneficial because natural force-free solutions are the most economical to maintain. Every solution is characterized by an initial condition. Therefore, we seek to find those initial conditions that lead to bounded solutions close to the circular orbit solutions.

Nonlinearity Without Eccentricity

In this section, we study the effect of nonlinearity on relative motion dynamics for a circular reference orbit. The governing differential equations are

$$\ddot{x} - 2n\dot{y} - n^2x = \frac{-\mu(a_c + x)}{\left[(a_c + x)^2 + y^2 + z^2\right]^{\frac{3}{2}}} + \frac{\mu}{a_c^2}$$
$$\ddot{y} + 2n\dot{x} - n^2y = \frac{-\mu y}{\left[(a_c + x)^2 + y^2 + z^2\right]^{\frac{3}{2}}}$$
$$\ddot{z} = \frac{-\mu z}{\left[(a_c + x)^2 + y^2 + z^2\right]^{\frac{3}{2}}} \quad (6)$$

where a_c is the semimajor axis of the chief and $n = \sqrt{(\mu/a_c^3)}$ is the mean motion of the chief. A Taylor's series expansion of the right-hand side (RHS) of Eqs. (6), retaining quadratic terms, leads to the following model:

$$\ddot{x} - 2n\dot{y} - 3n^2x = \left(3\mu/a_c^4\right)[y^2/2 + z^2/2 - x^2]$$
$$\ddot{y} + 2n\dot{x} = \left(3\mu/a_c^4\right)xy, \qquad \ddot{z} + n^2z = \left(3\mu/a_c^4\right)xz \quad (7)$$

This model can be considered as perturbed HCW equations with $\varepsilon = 3\mu/a_c^4$ the perturbation parameter.

Let x_h, y_h, and z_h be the solutions to the HCW equations, the unperturbed problem. We assume the solution to Eqs. (7) to be of the following form:

$$x = x_h + \varepsilon x_{cn}, \qquad \dot{x} = \dot{x}_h + \varepsilon\dot{x}_{cn}, \qquad \ddot{x} = \ddot{x}_h + \varepsilon\ddot{x}_{cn}$$
$$y = y_h + \varepsilon y_{cn}, \qquad \dot{y} = \dot{y}_h + \varepsilon\dot{y}_{cn}, \qquad \ddot{y} = \ddot{y}_h + \varepsilon\ddot{y}_{cn}$$
$$z = z_h + \varepsilon z_{cn}, \qquad \dot{z} = \dot{z}_{cn} + \varepsilon\dot{z}_{cn}, \qquad \ddot{z} = \ddot{z}_h + \varepsilon\ddot{z}_{cn} \quad (8)$$

The subscript h in the preceding equations refers to the solutions to the HCW equations and the subscript cn refers to the nonlinearity correction. The variables with the subscript cn are also referred to as the perturbation variables.

The HCW state vector and its initial value are represented as

$$\boldsymbol{X}_h(t) = [x_h(t) \quad y_h(t) \quad z_h(t) \quad \dot{x}_h(t) \quad \dot{y}_h(t) \quad \dot{z}_h(t)]^T$$
$$\boldsymbol{X}_h(0) = [x_h(0) \quad y_h(0) \quad z_h(0) \quad \dot{x}_h(0) \quad \dot{y}_h(0) \quad \dot{z}_h(0)]^T \quad (9)$$

The unperturbed solution, linear solution, and the HCW solution are completely equivalent in the present context. We choose the following HCW solution as shown earlier in Eq. (3) as $\boldsymbol{X}_h(t)$:

$$x_h = (\rho/2)\sin(nt+\alpha_0), \qquad y_h = \rho\cos(nt+\alpha_0)$$
$$z_h = \rho\sin(nt+\alpha_0), \qquad \dot{x}_h = (\rho/2)n\cos(nt+\alpha_0)$$
$$\dot{y}_h = -\rho n\sin(nt+\alpha_0), \qquad \dot{z}_h = \rho n\cos(nt+\alpha_0) \tag{10}$$

where ρ and α_0 are shown in Fig. 1. Note that the initial conditions for the HCW solutions are referred as HCW initial conditions. These are obtained by substituting $t=0$ in Eqs. (10):

$$\therefore \boldsymbol{X}_h(0) = [(\rho/2)\sin\alpha_0 \quad \rho\cos\alpha_0 \quad \rho\sin\alpha_0$$
$$(\rho/2)n\cos\alpha_0 \quad -\rho n\sin\alpha_0 \quad \rho n\cos\alpha_0]^T \tag{11}$$

The perturbation variables and the perturbation variable initial conditions are represented as

$$\boldsymbol{X}_{cn}(t) = [x_{cn}(t) \quad y_{cn}(t) \quad z_{cn}(t) \quad \dot{x}_{cn}(t) \quad \dot{y}_{cn}(t) \quad \dot{z}_{cn}(t)]^T$$
$$\boldsymbol{X}_{cn}(0) = [x_{cn}(0) \quad y_{cn}(0) \quad z_{cn}(0) \quad \dot{x}_{cn}(0) \quad \dot{y}_{cn}(0) \quad \dot{z}_{cn}(0)]^T \tag{12}$$

The initial conditions to the complete solution are

$$\boldsymbol{X}(0) = \boldsymbol{X}_h(0) + \varepsilon\boldsymbol{X}_{cn}(0) \tag{13}$$

Whereas the initial conditions for the HCW solution $\boldsymbol{X}_h(0)$ are predetermined, the initial conditions on the perturbation variables $\boldsymbol{X}_{cn}(0)$ are to be determined. If the initial conditions on the perturbation variables are not chosen properly, the resulting solutions will depart from the desired bounded HCW solutions, due to secular growth. The objective in this section is to show that the initial conditions on the perturbation variables can be chosen to eliminate the secular growth.

The following equations are obtained for the perturbation variables after substituting Eqs. (8) into Eqs. (7) and equating the coefficient of ε on both sides:

$$\ddot{x}_{cn} - 2n\dot{y}_{cn} - 3n^2x_{cn} = \left(y_h^2 + z_h^2 - 2x_h^2\right)/2$$
$$\ddot{y}_{cn} + 2n\dot{x}_{cn} = x_h y_h, \qquad \ddot{z}_{cn} + n^2 z_{cn} = x_h z_h \tag{14}$$

Substitution of Eqs. (10) into Eqs. (14) results in the following set of equations:

$$\ddot{x}_{cn} - 2n\dot{y}_{cn} - 3n^2x_{cn} = 3\rho^2/8 + (\rho^2/8)\cos(2nt+2\alpha_0)$$
$$\ddot{y}_{cn} + 2n\dot{x}_{cn} = (\rho^2/4)\sin(2nt+2\alpha_0)$$
$$\ddot{z}_{cn} + n^2 z_{cn} = \rho^2/4 - (\rho^2/4)\cos(2nt+2\alpha_0) \tag{15}$$

Equations (15) can be written in the form

$$\dot{\boldsymbol{X}}_{cn} = A_h\boldsymbol{X}_{cn} + B\boldsymbol{u}_h \tag{16}$$

where

$$A_h = \begin{bmatrix} 0 & 0 & 0 & 1 & 0 & 0 \\ 0 & 0 & 0 & 0 & 1 & 0 \\ 0 & 0 & 0 & 0 & 0 & 1 \\ 3n^2 & 0 & 0 & 0 & 2n & 0 \\ 0 & 0 & 0 & -2n & 0 & 0 \\ 0 & 0 & -n^2 & 0 & 0 & 0 \end{bmatrix}, \qquad \boldsymbol{X}_{cn} = \begin{bmatrix} x_{cn} \\ y_{cn} \\ z_{cn} \\ \dot{x}_{cn} \\ \dot{y}_{cn} \\ \dot{z}_{cn} \end{bmatrix}$$

$$B = \begin{bmatrix} 0 & 0 & 0 \\ 0 & 0 & 0 \\ 0 & 0 & 0 \\ 1 & 0 & 0 \\ 0 & 1 & 0 \\ 0 & 0 & 1 \end{bmatrix}, \qquad \boldsymbol{u}_h = \begin{bmatrix} \frac{3\rho^2}{8} + \frac{\rho^2}{8}\cos(2nt+2\alpha_0) \\ \frac{\rho^2}{4}\sin(2nt+2\alpha_0) \\ \frac{\rho^2}{4} - \frac{\rho^2}{4}\cos(2nt+2\alpha_0) \end{bmatrix}$$

Equations (16) are a set of linear constant coefficient nonhomogeneous ordinary differential equations. The state transition matrix for the homogeneous solution is same as the state transition matrix for the HCW equations, available in Ref. 12:

$$\Phi_h(t) = \begin{bmatrix} 4-3c & 0 & 0 & \frac{s}{n} & \frac{2}{n}(1-c) & 0 \\ 6(s-nt) & 1 & 0 & \frac{-2}{n}(1-c) & \frac{4s-3nt}{n} & 0 \\ 0 & 0 & c & 0 & 0 & \frac{s}{n} \\ 3ns & 0 & 0 & c & 2s & 0 \\ -6n(1-c) & 0 & 0 & -2s & 4c-3 & 0 \\ 0 & 0 & -ns & 0 & 0 & c \end{bmatrix} \tag{17}$$

where $c = \cos(nt)$ and $s = \sin(nt)$.

The general solution to Eqs. 16 can be written as

$$\boldsymbol{X}_{cn}(t) = \Phi_h(t)\boldsymbol{X}_{cn}(0) + \int_0^t \Phi_h(t-\tau)B\boldsymbol{u}_h(\tau)\,\mathrm{d}\tau \tag{18}$$

from which the following results for the scalar position components of $\boldsymbol{X}_{cn}(t)$ can be derived as

$$x_{cn}(t) = [4-3\cos nt]x_{cn}(0) + \frac{\sin nt}{n}\dot{x}_{cn}(0) + 2\frac{1-\cos nt}{n}\dot{y}_{cn}(0) + \frac{1}{48}\frac{\rho^2[18+12\cos 2\alpha_0]}{n^2}$$
$$+ \frac{1}{48}\frac{\rho^2[2\cos(2nt+2\alpha_0) - 5\cos(nt-2\alpha_0) - 9\cos(nt+2\alpha_0) - 18\cos nt]}{n^2} \tag{19}$$

$$y_{cn}(t) = [6\sin nt - 6nt]x_{cn}(0) + y_{cn}(0) - 2\frac{1-\cos nt}{n}\dot{x}_{cn}(0) + \frac{4\sin nt - 3nt}{n}\dot{y}_{cn}(0) - \frac{1}{48}\frac{\rho^2[36nt + 18nt\cos(2\alpha_0)]}{n^2}$$
$$- \frac{1}{48}\frac{\rho^2[5\sin(2nt+2\alpha_0) + 3\sin 2\alpha_0 - 18\sin(nt+2\alpha_0) - 10\sin(nt-2\alpha_0) - 36\sin nt]}{n^2} \tag{20}$$

$$z_{cn}(t) = \cos nt\, z_{cn}(0) + \frac{\sin nt}{n}\dot{z}_{cn}(0) + \frac{1}{24}\frac{\rho^2[6]}{n^2}\frac{1}{24}\frac{\rho^2[2\cos(2nt+2\alpha_0) - 6\cos nt + \cos(nt-2\alpha_0) - 3\cos(nt+2\alpha_0)]}{n^2} \tag{21}$$

It is clear from the preceding expressions that no choice of initial conditions will make all of the perturbation variables vanish. There are three types of terms in these expressions: 1) constant bias terms, 2) secular terms, and 3) harmonic terms. The secular terms are of serious concern because they can cause unbounded departure of the nonlinear solution from the HCW solutions. The secular terms only appear in the along-track direction y. Therefore, a weak criterion for zero secular growth for the nonlinear problem is

$$\left\{-6nx_{cn}(0) - 3\dot{y}_{cn}(0) - \tfrac{1}{48}\left[\rho^2(36n + 18n\cos 2\alpha_0)\right]/n^2\right\} = 0 \tag{22}$$

The preceding criterion is referred to as a weak criterion because it results from an approximate solution (first-order perturbation solution) to an approximate model (with quadratic nonlinearities only) to the true nonlinear problem. The following arbitrary choice of perturbation variable initial conditions satisfy the specified criterion:

$$x_{cn}(0) = 0, \qquad \dot{y}_{cn}(0) = -(\rho^2/48n)(12 + 6\cos 2\alpha_0) \tag{23}$$

Hence, the desired initial perturbation state vector is

$$\boldsymbol{X}_{cn}(0) = \left[0 \;\; 0 \;\; 0 \;\; 0 \;\; (-\rho^2/48n)(12 + 6\cos 2\alpha_0) \;\; 0\right]^T \tag{24}$$

This initial condition correction will be referred to as basic nonlinearity correction in the rest of the paper.

The preceding choice is just one of the infinite combinations of $x_{cn}(0)$ and $\dot{y}_{cn}(0)$ that satisfy the zero secular growth requirement.

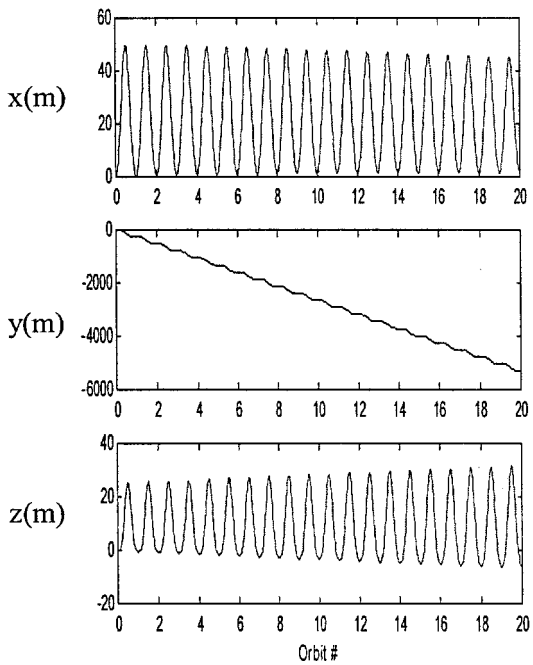

Fig. 2a Deviation of nonlinear simulation from HCW solution with Hill's ICs, α_0 = 0 deg.

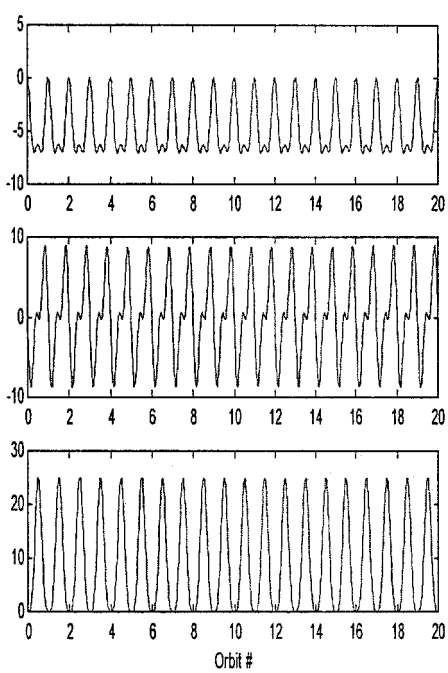

Fig. 2b Deviation of nonlinear simulation from HCW solution with corrected ICs, α_0 = 0 deg.

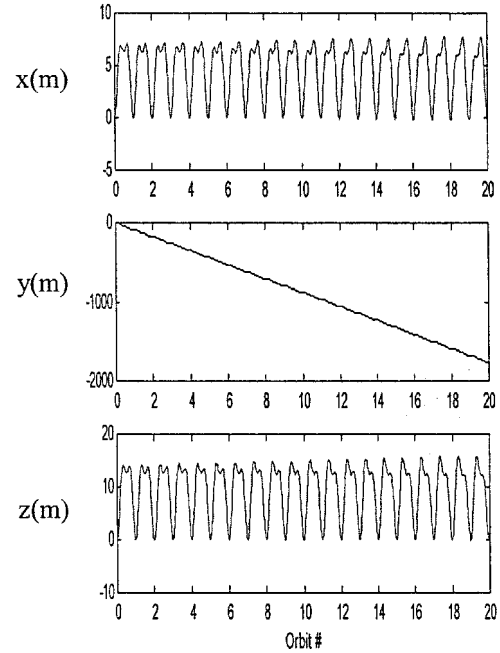

Fig. 3a Deviation of nonlinear simulation from HCW solution with Hill's ICs, α_0 = 90 deg.

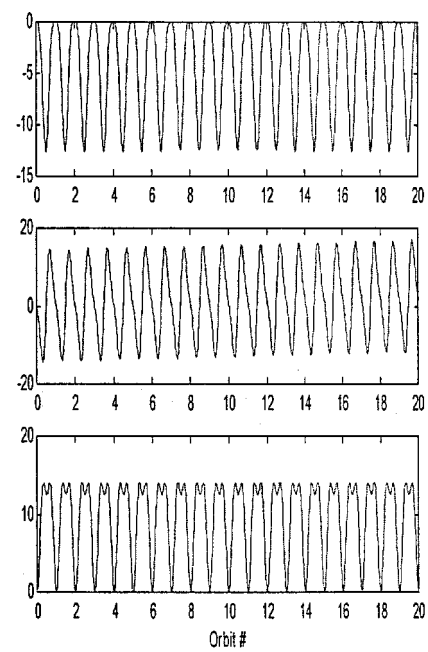

Fig. 3b Deviation of nonlinear simulation from HCW solution with corrected ICs, α_0 = 90 deg.

Note that the initial conditions on the remaining perturbation variables could also be chosen to eliminate some of the biases and the harmonic terms appearing in the x_{cn} and z_{cn} solutions.

The effectiveness of this correction is tested on Eqs. (6). The plots in Fig. 2 are the results of simulations conducted on Eqs. (6) with the parameters: $a_c = 8000$ km, $\rho = 10$ km, $\alpha_0 = 0$ deg, 90 deg, and $e = 0$. Figures 2a and 2b show the deviation from the HCW projected circular orbit solution with and without the nonlinearity correction, respectively, for the $\alpha_0 = 0$ deg deputy. Note that the correction brings down to almost zero an otherwise secular growth of 260 m/orbit. Shown in Figs. 3a and 3b are similar plots for the $\alpha_0 = 90$ deg satellite.

The complete solution to the nonlinear problem is

$$\boldsymbol{X}(t) = \Phi_h(t)\boldsymbol{X}_h(0) + \Phi_h(t)\varepsilon\boldsymbol{X}_{cn}(0) + \varepsilon\int_0^t \Phi_h(t-\tau)B\boldsymbol{u}_h(\tau)\,\mathrm{d}\tau \tag{25}$$

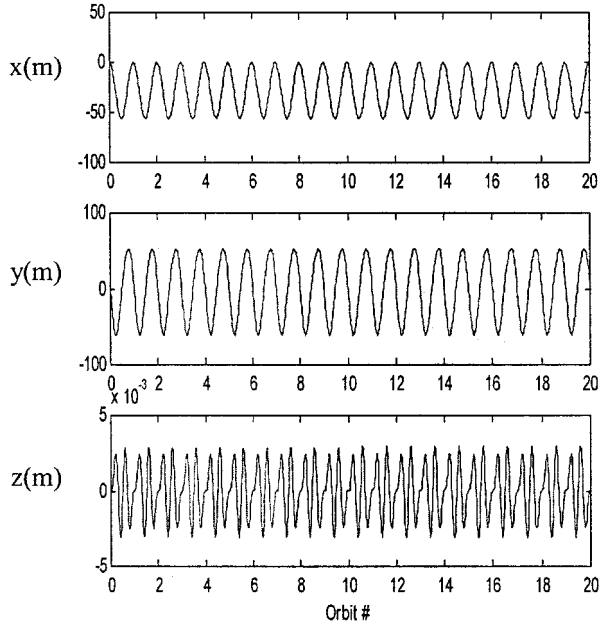

Fig. 4a Validity of perturbation solution with corrected ICs for α_0 = 0 deg.

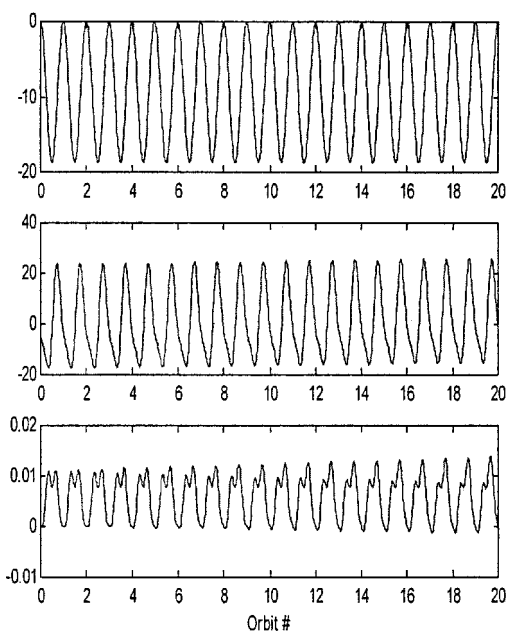

Fig. 4b Validity of perturbation solution with corrected ICs for α_0 = 90 deg.

The validity of the perturbation solution with the corrected initial conditions is shown in Figs. 4a and 4b for the 0- and the 90-deg satellites, respectively. The deviations from the exact numerical results are bounded for both of the deputies. There are small but constant offsets from Hill's solutions in Figs. 2a and 3a in the x and z directions. The perturbation solution captures the bias term in the x direction partially, but it captures the bias term in the z direction very accurately, as can be seen from the Figs. 4a and 4b.

Period Matching

In the absence of any disturbances and perturbations, two satellites in Keplerian orbits can have bounded relative motion only when their periods match. This requires the semimajor axes of both the satellites be the same. The relative motion initial conditions along with the chief's initial conditions determine the orbital elements of the deputy. In this section, we shall relate the nonlinearity correction to the period-matching requirement.

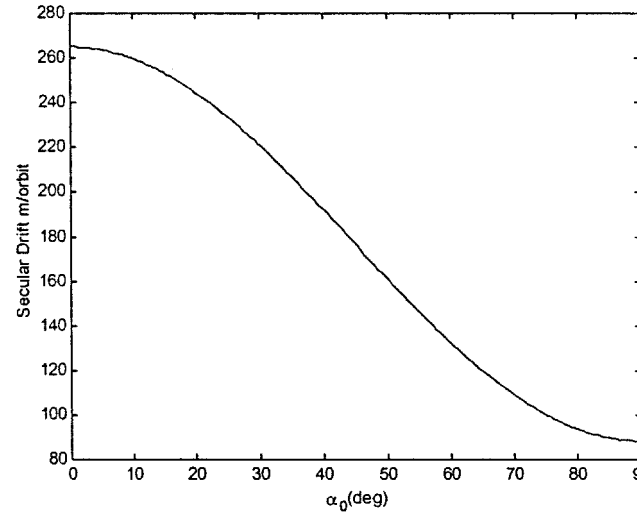

Fig. 5a Secular drift prediction based on δa computation with HCW ICs.

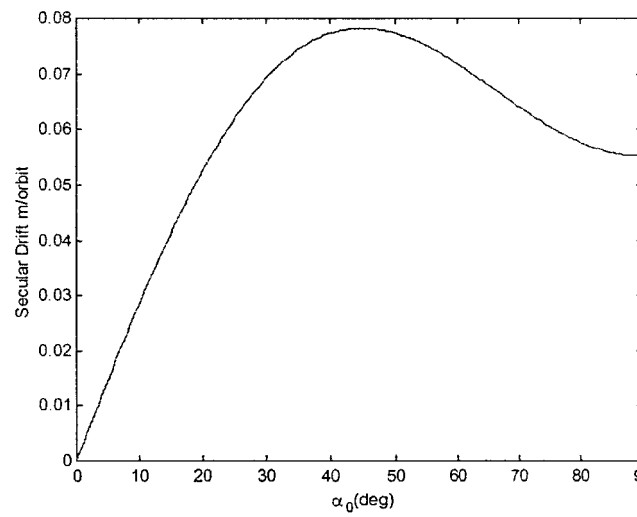

Fig. 5b Secular drift prediction based on δa computation with corrected ICs.

The semimajor axis of a deputy is computed using the initial conditions on the chief and the relative motion initial conditions with and without the correction. First, the relative motion initial conditions are transformed from the LVLH frame to the inertial frame. The transformed quantities are added to the inertial coordinates of the chief to obtain the inertial coordinates of the deputy. Then the semimajor axis is obtained by converting the inertial coordinates of the deputy to orbital elements. It can be shown that a semimajor axes difference of δa results in approximately a secular drift of $-3\pi\delta a$/orbit. Shown in Figs. 5a and 5b are the secular drift predictions based on δa computation with and without the basic nonlinearity correction, respectively. The secular drift is plotted as a function of α_0 of the deputy. Figure 5a shows the secular growth predicted with HCW initial conditions, that is, without the basic nonlinearity correction. The secular growth prediction varies from a maximum of 265 m/orbit for the $\alpha_0 = 0$ deg satellite to a minimum of 85 m/orbit for the $\alpha_0 = 90$ deg deputy satellite. Figures 2a and 3a confirm these predictions both qualitatively and quantitatively. Also, the basic nonlinearity correction term, which is a function of α_0, assumes a maximum value for $\alpha_0 = 0$ and 180 deg and a minimum value for $\alpha_0 = 90$ and 270 deg. The secular drifts in Fig. 5b with the nonlinearity corrected initial conditions are much smaller. It can be seen that the nonlinearity correction enforces the period-matching requirement. Matching the periods is of cardinal importance for bounded relative motion. HCW initial conditions do not result in

deputy orbits with the same semimajor axis as that of the chief. The nonlinearity corrected initial conditions result in orbits with much smaller δa. Hence, they result in much smaller secular drifts. The secular growth resulting from the corrected initial conditions is not exactly zero because the correction is made considering terms only up to first order and nonlinearities only up to quadratic terms.

Linearized Dynamics with Eccentricity Effects

In this section, we study the effect of eccentricity on HCW solutions. In the preceding two sections, we studied the effect of nonlinearity in the absence of eccentricity. In this section, we study the effect of eccentricity in the absence of nonlinearity. The governing differential equations are given in Eqs. (26). We will be primarily concerned with condition for bounded solutions of Eqs. (26) and the solution representation. A condition for bounded relative orbit to Eqs. (26) was derived by Inalhan et al.[2] and is given in Eq. (27). This results from a solution to Eqs. (26) in nondimensional variables and with true anomaly as the independent variable. Different researchers have obtained the solution to Eqs. (26), but only Melton[1] has a time-explicit solution to these equations. Hence, we adopt Melton's state transition matrix solution for representing the bounded relative orbit solution:

$$\ddot{x} - 2\dot{\theta}\dot{y} - \ddot{\theta}y - \dot{\theta}^2 x - 2\left(\mu/r_c^3\right)x = 0$$

$$\ddot{y} + 2\dot{\theta}\dot{x} + \ddot{\theta}x - \dot{\theta}^2 y + \left(\mu/r_c^3\right)y = 0$$

$$\ddot{z} + \left(\mu/r_c^3\right)z = 0, \qquad \ddot{r}_c = r_c\dot{\theta}^2 - \mu/r_c^2, \qquad \ddot{\theta} = -(2\dot{r}_c\dot{\theta}/r_c) \tag{26}$$

The bounded relative orbit condition when the chief is at the perigee at the initial time is

$$\dot{y}_0/x_0 = -\left[n(2+e)/(1+e)^{\frac{1}{2}}(1-e)^{\frac{3}{2}}\right] \tag{27}$$

For $e = 0$, the condition reduces to $\dot{y}_0 + 2nx_0 = 0$, which is the condition for bounded relative orbit solutions to HCW equations. Therefore, the earlier criterion can be used to derive a correction to the $\dot{y}_0$ HCW initial condition, which results in bounded orbits close to the HCW solutions. The correction could alternatively be derived on the x_0 initial condition as well. The correction $\delta(e)$ on $\dot{y}_0$ is computed as follows:

$$\dot{y}_0 = -\rho n \sin\alpha_0 + \delta(e) \tag{28}$$

Plugging Eq. (28) into Eq. (27) and taking $x_0 = (\rho/2)\sin\alpha_0$, we can solve for $\delta(e)$,

$$\delta(e) = n\rho\sin\alpha_0\left\{1 - \left[(2+e)/2(1+e)^{\frac{1}{2}}(1-e)^{\frac{3}{2}}\right]\right\} \tag{29}$$

The preceding correction to $\dot{y}_0$ will be referred to as the linearized eccentricity correction for the rest of the paper. This correction is a function of eccentricity and becomes zero for $e = 0$. The correction to HCW initial conditions has been found to result in perfectly bounded orbits from the integration of Eqs. (26). In contrast to the basic nonlinearity correction, which is a first-order correction, this is an exact correction to obtain bounded relative orbits from Eqs. (26). A closer look at Eq. (29) shows that the effect of eccentricity is maximum for the $\alpha_0 = 90$ deg deputy and zero for the $\alpha_0 = 0$ deg deputy. Note that this bounded relative orbit criterion could also be derived by using the geometric approach of Alfriend et al.[8] and the state transition matrix solution of Melton.[1] A derivation of the bounded relative orbit criterion using the geometric approach is given in the Appendix. The result derived is applicable for all initial positions of the chief and is not restricted to the perigee. Whereas the condition can be exactly derived using the Alfriend et al.[8] geometric approach, only a weaker version of it can be derived using Melton's state transition matrix. This is because Melton's state transition matrix is obtained in terms of a series expansion of eccentricity. Therefore, the secular growth can be captured only to e^2 terms (as computed by Melton).

Also, Melton's[1] state transition matrix solution contains secular terms in the x direction that are unexpected. Therefore, for higher values of eccentricity, the solution obtained is not very accurate. The accuracy of the solution improves by computing the solution until e^3 terms for x and y. It is expected that, as we go to higher orders, the secular terms cancel each other in the x direction, and the secular terms in the y direction account for the secular growth that results due to the violation of Eq. (27). Therefore, to get a time-explicit representation for the bounded relative motion obtained by making the linearized eccentricity correction, we drop all of the secular terms in x and y directions in Melton's state transition matrix. Melton's state transition matrix solution captures the bias terms and higher-order harmonics very accurately. The solution, retaining just the constant and harmonic terms is

$$\begin{aligned}
x_{\mathrm{le}}(t) &= [(4 - 3cnt) + (-5cnt - 3c2nt + 13 - 5cnt)e \\
&\quad + (40 - 40c2nt - -40cnt - 27c3nt - 24c2nt \\
&\quad + 152 - 61cnt)e^2/8 + (-33/4c3nt - 7c2nt - 55/4cnt \\
&\quad - 4c4nt + 33)e^3]x_0 + [snt/n + (-3snt + s2nt + snt)e/n \\
&\quad + (-4snt + 8s2nt + 9s3nt - 24s2nt + 9snt)e^2/(8n) \\
&\quad + (16s4nt + 9snt + 4s2nt - 27s3nt)e^3/(12n)]\dot{x}_0 \\
&\quad + [(2snt - 4s2nt + 7snt + 4s2nt - 9snt)e^2/4]y_0 \\
&\quad + [2(1 - cnt)/n + (8 - 4cnt - 4c2nt)e/(2n) \\
&\quad + (8 - 5cnt - 4c2nt - 9c3nt)e^2/(4n) - (-24 - 64c2nt \\
&\quad + 6cnt + 18c3nt + 64c4nt)e^3/(24n)]\dot{y}_0
\end{aligned} \tag{30}$$

$$\begin{aligned}
y_{\mathrm{le}}(t) &= [6snt + (4snt + 9s2nt + 20snt)e/2 \\
&\quad + (42snt + 36s2nt + 18s3nt)e^2/4 \\
&\quad + (9snt + 23/4s2nt + 9s3nt + 5s4nt)e^3]x_0 \\
&\quad + [1 + (1 - cnt)e + (3 - 2cnt - c2nt)e^2/2 \\
&\quad + (-5/8cnt - 1/2c2nt - 3/8c3nt + 3/2)e^3]y_0 \\
&\quad + [-2/n(1 - cnt) + (-4cnt + 3c2nt + 1)e/(2n) \\
&\quad + (4 - 2cnt - 8c2nt + 6c3nt)e^2/(4n) + (-5c2nt \\
&\quad + 15cnt - 27c3nt + 20c4nt - 3)e^3/(12n)]\dot{x}_0 \\
&\quad + [4snt/n + 3es2nt/n + (-12snt + 12s3nt)e^2/(4n) \\
&\quad + (-88s2nt + 80s4nt)e^3/24/n]\dot{y}_0
\end{aligned} \tag{31}$$

$$\begin{aligned}
z_{\mathrm{le}}(t) &= [cnt + (c2nt/2 - 3/2 + cnt)e \\
&\quad + (5cnt + 4c2nt + 3c3nt - 12)e^2/8]z_0 \\
&\quad + [snt/n + (-2snt + s2nt)e/(2n) \\
&\quad + (-4snt + 2s2nt + 3s3nt - 6s2nt + 3snt)e^2/(8n)]\dot{z}_0
\end{aligned} \tag{32}$$

and $cjnt = \cos(njt)$ and $sjnt = \sin(njt)$, where subscript le refers to the linearized problem with eccentricity.

Note that the preceding solution is valid only for the eccentricity corrected initial conditions. The maximum error incurred between the preceding approximate solution and the numerical integration of Eqs. (26) is less than 0.3% of the disk size for an eccentricity of $e = 0.1$. Also, the solution is valid for the initial position of the chief being its perigee, that is, the time of perigee passage $t_p = 0$.

Bias Correction

Although the eccentricity correction results in bounded orbits, it does not lead to relative orbits that are exactly circular in the y–z plane. It can be seen from Eqs. (31) and (32) that there are significant

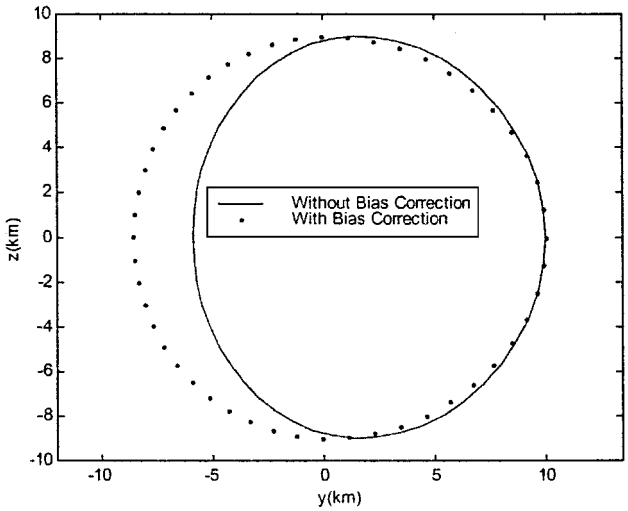

Fig. 6 Relative orbit for $\alpha_0 = 0$ deg deputy obtained with and without bias correction.

bias terms in the y and the z directions. These terms offset the relative orbit with respect to the chief. The bias term along the y direction can be eliminated by making a correction to the $\dot{x}_0$ initial condition or the y_0 initial condition. The following corrected $\dot{x}_0$ initial condition is obtained to cancel the bias term in y direction:

$$\dot{x}_0 = n(\rho/2)\sin\alpha_0 + \rho en\cos\alpha_0[(8e+5)/(8-2e-4e^2)] \quad (33)$$

The correction (33) has been derived by isolating the bias terms in Eq. (31). The bias is maximum for the $\alpha_0 = 0$ deg deputy and minimum for the $\alpha_0 = 90$ deg deputy. Figure 6 demonstrates the benefit of the bias correction. The solid line is the relative orbit obtained by integrating Eqs. (26) with the eccentricity correction alone. It can be seen that the orbit is bounded but not symmetric about the chief. The dotted line represents the relative orbit obtained with both the linearized eccentricity correction and the bias correction. It can be seen that the bias corrected relative orbit is more symmetric about the chief.

The bias correction and the linearized eccentricity correction are independent of each other. Whereas the linearized eccentricity correction depends on x_0 and $\dot{y}_0$, the bias correction depends on y_0 and $\dot{x}_0$. Note that the eccentricity correction and the bias correction to the relative motion initial conditions given in this section are for the initial location of the chief being its perigee.

Combining the Effects of Nonlinearity and Eccentricity

The preceding two sections addressed the problem of eccentricity without nonlinearity. The sections before those addressed the problem of nonlinearity in the absence of eccentricity. The main problem consists of both the effects acting together. Neither of the corrections derived produce bounded solutions from the complete nonlinear simulation for an eccentric reference orbit. In this section, we look at the solution to the combined problem and derive the corresponding conditions for bounded solutions. The approach is similar to the perturbation technique adopted earlier for the nonlinear problem without eccentricity.

The linearized dynamics with eccentricity, which is given by Eqs. (26), can be written using series expansions[1] for r_c, $\dot{\theta}$, and $\ddot{\theta}$ as

$$\dot{\boldsymbol{X}} = A(t)\boldsymbol{X} \quad (34)$$

where $A(t) = A_h + eA_{1e} + e^2A_{2e} + \cdots$. Adding the quadratic nonlinearities as shown in Eqs. (5) results in the perturbed problem

$$\dot{\boldsymbol{X}} = A(t)\boldsymbol{X} + \varepsilon\boldsymbol{f}(\boldsymbol{X}) \quad (35)$$

where ε is the perturbation parameter and $\boldsymbol{f}(\boldsymbol{X})$ represents the quadratic nonlinearities, terms on the RHS of Eqs. (5).

The solution to the perturbed problem is assumed to be of the form

$$\boldsymbol{X} = \boldsymbol{X}_{\text{le}} + \varepsilon\boldsymbol{X}_1 \quad (36)$$

where $\boldsymbol{X}_{\text{le}}$ is the solution to linearized problem with eccentricity given by Eqs. (34). Substituting expression (36) in the perturbed form of the linearized equations with eccentricity, we get the following differential equations for the perturbation variables $\boldsymbol{X}_1$:

$$\dot{\boldsymbol{X}}_1 = A(t)\boldsymbol{X}_1 + \boldsymbol{f}(\boldsymbol{X}_{\text{le}}) \quad (37)$$

The solution to the linearized problem with eccentricity effects, for the eccentricity corrected initial conditions can be written as

$$\boldsymbol{X}_{\text{le}} = \boldsymbol{X}_h + e\boldsymbol{X}_{1e} + e^2\boldsymbol{X}_{2e} + \cdots \quad (38)$$

Terms up to e^3 in the $\boldsymbol{X}_{\text{le}}$ series expansion are given by Eqs. (30–32).

$\boldsymbol{X}_{\text{le}}$ forms the zeroth-order solution to Eqs. (35). Note the first term in the preceding series represents the HCW solution. The state transition matrix to the linearized problem with eccentricity can also be written[1] as

$$\Phi_{\text{le}} = \Phi_h + e\Phi_{1e} + e^2\Phi_{2e} + \cdots \quad (39)$$

Again, the first term in the series is the state transition matrix to HCW equations.

The forcing function in Eq. (37) can be written as follows:

$$\boldsymbol{f}(\boldsymbol{X}_{\text{le}}) = B\boldsymbol{u}$$

where B is 6×3 matrix and $\boldsymbol{u}$ is a 3×1 vector,

$$\boldsymbol{u} = \boldsymbol{u}_h + e\boldsymbol{u}_1 + e^2\boldsymbol{u}_2 + \cdots \quad (40)$$

Substituting Eq. (40) into Eq. (37), we get

$$\therefore \dot{\boldsymbol{X}}_1 = A(t)X_1 + \varepsilon B\boldsymbol{u} \quad (41)$$

The solution to this problem can be written as

$$\boldsymbol{X}_1(t) = \Phi(t)\boldsymbol{X}_1(0) + \int_0^t \Phi(t-\tau)B\boldsymbol{u}(\tau)\,\mathrm{d}\tau$$

and the overall solution would be

$$\boldsymbol{X}(t) = \boldsymbol{X}_{\text{le}}(t) + \varepsilon\Phi(t)\boldsymbol{X}_1(0) + \varepsilon\int_0^t \Phi(t-\tau)B\boldsymbol{u}(\tau)\,\mathrm{d}\tau$$

$$= \boldsymbol{X}_{\text{le}}(t) + \varepsilon\Phi(t)\boldsymbol{X}_1(0) + \varepsilon\Phi(t)\int_0^t [\Phi_h(-\tau) + e\Phi_{1e}(-\tau) + \cdots]B[\boldsymbol{u}_h(\tau) + e\boldsymbol{u}_1(\tau) + \cdots]\,\mathrm{d}\tau \quad (42)$$

$\boldsymbol{X}_{\text{le}}(t)$ is a bounded solution and the terms appearing to the right of it in expression (42) are a result of the nonlinear perturbation. There are two perturbations in the preceding solution, 1) the nonlinearity perturbation ε and 2) the eccentricity perturbation e. The terms containing the product of these parameters can be neglected for values of eccentricity less than 0.1. The solution retaining the largest terms from the perturbation solution can be written as follows:

$$\boldsymbol{X}(t) = \boldsymbol{X}_{\text{le}}(t) + \varepsilon\Phi(t)\boldsymbol{X}_1(0) + \varepsilon\Phi_h(t)\int_0^t \Phi_h(-\tau)B\boldsymbol{u}_h(\tau)\,\mathrm{d}\tau \quad (43)$$

Note that the only perturbation terms remaining in expression (43) are the nonlinearity perturbation terms resulting for the circular reference orbit problem. Therefore, a first-order solution to the nonlinear problem with eccentricity, considering just the circular orbit nonlinearity effects is

$$X(t) = X_{\text{le}}(t) + \varepsilon X_{cn}(t) \quad (44)$$

Bounded solutions to $X(t)$ require choosing another correction to the eccentricity corrected initial conditions to eliminate secular

growth from the perturbation variables in Eq. (44). This correction would be the same as the nonlinearity correction for the circular reference orbit because all of the terms containing the product of eccentricity and nonlinearity parameter have been neglected. Therefore, two corrections are to be made to Hill's initial conditions to obtain bounded relative orbit solutions for the nonlinear problem with nonzero eccentricity. The first correction is the linearized eccentricity correction and the second term is the basic nonlinearity correction. Both these corrections are made to the $\dot{y}(0)$ initial condition. Combining the two corrections, we obtain the following initial condition for $\dot{y}(0)$:

$$\dot{y}(0) = -\rho n \sin\alpha_0 + \delta(e) + \varepsilon \dot{y}_{cn}(0) \tag{45}$$

where $\dot{y}_{cn}(0)$ is the same as the circular orbit nonlinearity correction given by Eq. (23).

Results

The following simulations demonstrate the effectiveness of the nonlinearity correction for the nonlinear eccentricity problem. Note that the following simulations are conducted on the complete nonlinear model given by Eqs. (1). The initial conditions are the same as Hill's initial conditions on all of the variables except for $\dot{y}(0)$ and $\dot{x}(0)$. The initial condition on $\dot{x}(0)$ has been corrected as per Eq. (33) to eliminate the bias in the y direction. Figures 7 and 8 show the relative orbits obtained with and without the basic nonlinearity correction on the $\dot{y}(0)$ initial condition. The broken lines in both Figs. 7 and 8 represent the relative orbits obtained with just the linearized eccentricity correction, and the solid line represents the relative orbit obtained with both the linearized eccentricity correction as well as the basic nonlinearity correction. The semimajor axis of the chief has been chosen to be 8000 km and the disk size 10 km. The simulation is conducted for 20 orbits.

Figures 9–12 show the secular drift in the y direction at the end of 20 orbits, with respect to the disk size for different satellites and different eccentricities, with and without the basic nonlinearity correction. It can be seen from Figs. 7–12 that some secular growth still exists in the y direction. This is due to the nonlinearity effects from the higher-order eccentricity terms. For higher values of eccentricity, one has to take the higher powers of eccentricity in Eq. (42) into consideration for the correction term.

Note that the eccentricity correction derived in Ref. 2 has a more significant effect on the drift rate than the nonlinearity correction. The secular drift resulting from not correcting for eccentricity is much higher than that resulting from not correcting for nonlinearity. However, both of these corrections are important for minimizing secular drift.

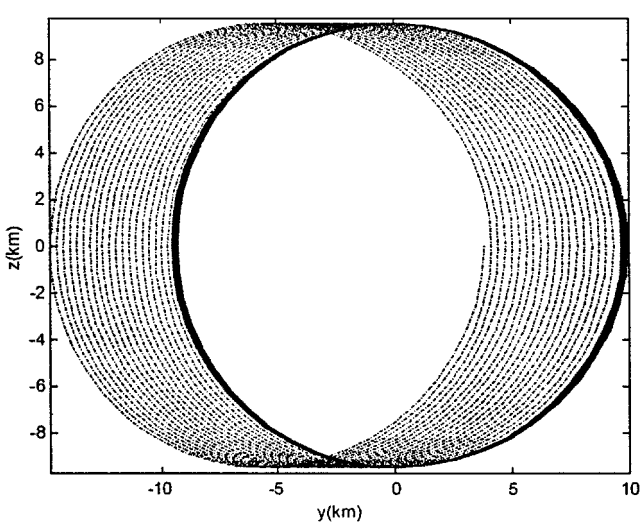

Fig. 7 Relative orbit with and without nonlinearity correction α_0 = 0 deg and e = 0.05.

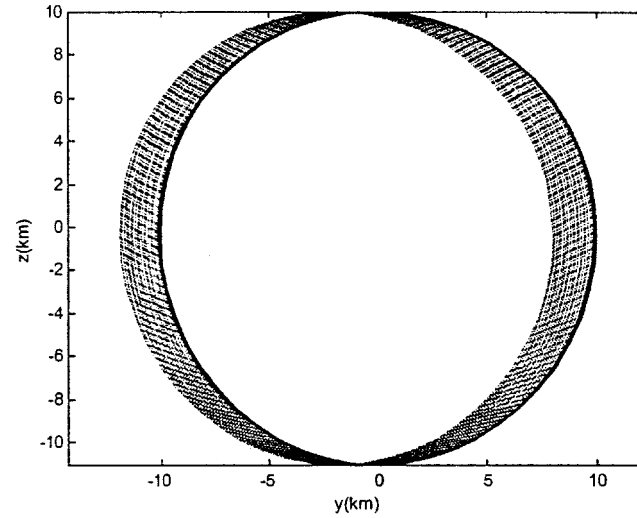

Fig. 8 Relative orbit with and without nonlinearity correction α_0 = 90 deg and e = 0.05.

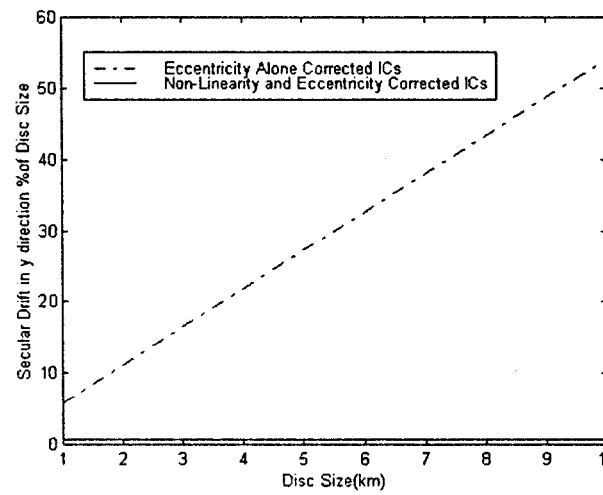

Fig. 9 Secular drift along y direction at the end of 20 orbits with and without nonlinearity correction, α_0 = 0 deg and e = 0.005.

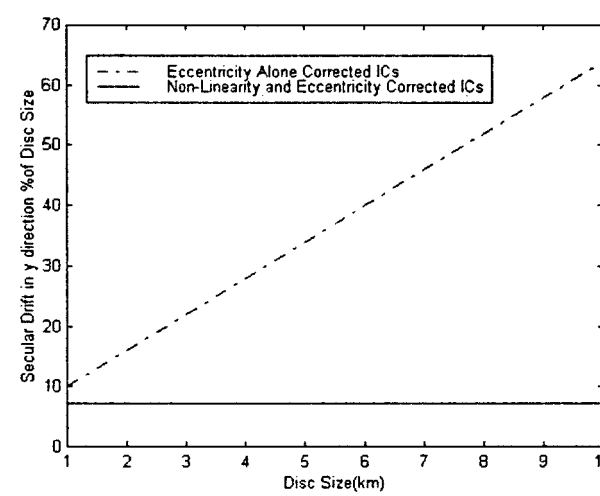

Fig. 10 Secular drift along y direction at the end of 20 orbits with and without nonlinearity correction, α_0 = 0 deg and e = 0.05.

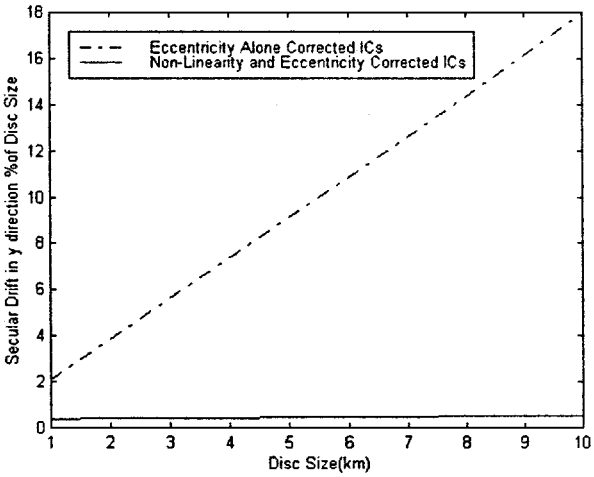

Fig. 11 Secular drift along y direction at the end of 20 orbits with and without nonlinearity correction, $\alpha_0 = 90$ deg and $e = 0.005$.

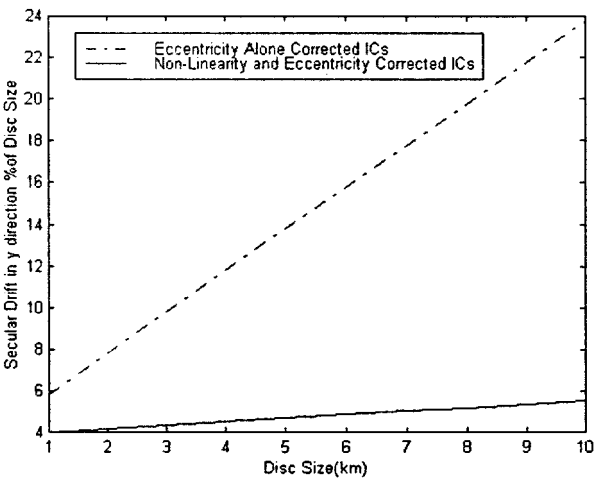

Fig. 12 Secular drift along y direction at the end of 20 orbits with and without nonlinearity correction, $\alpha_0 = 90$ deg and $e = 0.05$.

Conclusions

Time-explicit bounded solutions have been obtained for the relative motion problem accommodating the effects of eccentricity and quadratic nonlinear terms. The solution is obtained by combining the solutions to two different problems: 1) the nonlinear problem without eccentricity and 2) the linearized problem with eccentricity. The solution has been used to generate a correction to Hill's initial conditions. The correction has been related to the period-matching requirement for bounded relative motion. A bias correction has also been obtained to eliminate the bias in the y direction and better shape the relative orbit.

Appendix: Generalized Eccentricity Correction

The relationship between the linearized semimajor axis difference and the relative motion coordinates is given by the relation[8]

$$\delta a = A_{11}^{-1}x + A_{12}^{-1}\dot{x} + A_{13}^{-1}y + A_{14}^{-1}\dot{y} + A_{15}^{-1}z + A_{16}^{-1}\dot{z} \qquad \text{(A1)}$$

where A_{ij} are the elements of the geometric transformation matrix between the incremental orbital element differences and the relative motion coordinates

$$A_{11}^{-1} = -(V_t a\dot{\theta}/E)(1 + r_c/p_c), \qquad A_{12}^{-1} = -(V_r a/E)$$

$$A_{13}^{-1} = V_r a\dot{\theta}/E, \qquad A_{14}^{-1} = -(V_t a/E), \qquad A_{15}^{-1} = A_{16}^{-1} = 0 \qquad \text{(A2)}$$

where V_t is the transverse velocity of the chief and V_r is the radial velocity. Here p_c is the semilatus rectum of the chief and E is the energy of the chief,

$$V_t = r_c\dot{\theta} = p_c/(1 + e\cos f)\sqrt{(\mu/p_c^3)}(1 + e\cos f)^2$$

$$= \sqrt{(\mu/p_c)}(1 + e\cos f) \qquad \text{(A3)}$$

where f is the true anomaly of the chief

$$V_r = \dot{r}_c = e\sqrt{(\mu/p)}\sin f \qquad \text{(A4)}$$

$$\dot{\theta} = \sqrt{(\mu/p_c^3)}(1 + e\cos f)^2 \qquad \text{(A5)}$$

$$r_c = p_c/(1 + e\cos f) \qquad \text{(A6)}$$

Applying Eq. (A1) at time $t = 0$, we get the following constraint on ICs for zero linearized semimajor axis difference,

$$-V_t\dot{\theta}(1 + r_c/p)x_0 - V_r\dot{x}_0 + V_r\dot{\theta}y_0 - V_t\dot{y}_0 = 0 \qquad \text{(A7)}$$

$$\Rightarrow -\sqrt{(\mu/p)}(1 + e\cos f)\sqrt{(\mu/p^3)}(1 + e\cos f)^2$$

$$\times [1 + 1/(1 + e\cos f)]x_0 - e\sqrt{(\mu/p)}\sin f\,\dot{x}_0$$

$$+ e\sqrt{(\mu/p)}\sin f\sqrt{(\mu/p^3)}(1 + e\cos f)^2 y_0$$

$$- \sqrt{(\mu/p)}(1 + e\cos f)\dot{y}_0 = 0 \qquad \text{(A8)}$$

$$\Rightarrow -\sqrt{(\mu/p^3)}(1 + e\cos f)^3[1 + 1/(1 + e\cos f)]x_0 - e\sin f\,\dot{x}_0$$

$$+ e\sin f\sqrt{(\mu/p^3)}(1 + e\cos f)^2 y_0 - (1 + e\cos f)\dot{y}_0 = 0 \qquad \text{(A9)}$$

Equation (A9) is the generalized condition for zero secular growth from Eqs. 26. It can be used for any initial position of the chief. It involves all four initial conditions x_0, $\dot{x}_0$, y_0, and $\dot{y}_0$.

When the chief is at the perigee $f = 0$, substituting this into Eq. (A9), we get

$$\Rightarrow -\sqrt{\frac{\mu}{p^3}}(1 + e)^3\left(\frac{2 + e}{1 + e}\right)x_0 - (1 + e)\dot{y}_0 = 0 \qquad \text{(A10)}$$

$$\Rightarrow \frac{\dot{y}_0}{x_0} = -\sqrt{\frac{\mu}{p^3}}(1 + e)^2\left(\frac{2 + e}{1 + e}\right) = -\frac{n}{(1 - e^2)^{\frac{3}{2}}}\frac{(1 + e)^2(2 + e)}{(1 + e)}$$

$$= -n\frac{(2 + e)}{(1 + e)^{\frac{1}{2}}(1 - e)^{\frac{3}{2}}} \qquad \text{(A11)}$$

Note that Eq. (A11) is exactly same as Eq. 27.

Acknowledgments

The research was supported by Air Force Office of Scientific Research Grant F49620-01-1-0518 and NASA Grant NAG5-11349.

References

[1] Melton, R. G., "Time Explicit Representation of Relative Motion Between Elliptical Orbits," *Journal of Guidance, Control, and Dynamics*, Vol. 23, No. 4, 2000, pp. 604–610.

[2] Inalhan, G., Tillerson, M., and How, J. P., "Relative Dynamics and Control of Spacecraft Formations in Eccentric Orbits," *Journal of Guidance, Control, and Dynamics*, Vol. 25, No. 1, 2002, pp. 48–59.

[3] Anthony, M. L., and Sasaki, F. T., "Rendezvous Problem for Nearly Circular Orbits," *AIAA Journal*, Vol. 3, No. 9, 1965, pp. 1666–1673.

[4] Knollman, G. C., and Pyron, B. O., "Relative Trajectories of Objects Ejected from a Near Satellite," *AIAA Journal*, Vol. 1, No. 2, 1963, pp. 424–429.

[5] de Vries, J. P., "Elliptic Elements in Terms of Small Increments of Position and Velocity Components," *AIAA Journal*, Vol. 1, No. 11, 1963, pp. 2626–2629.

[6]London, H. S., "Second Approximation to the Solution of Rendezvous Equations," *AIAA Journal*, Vol. 1, No. 7, 1963, pp. 1691–1693.

[7]Karlgaard, C. D., and Lutze, F. H., "Second-Order Relative Motion Equations," American Astronautical Society, AAS Paper 01-474, July–Aug. 2001.

[8]Alfriend, K. T., Schaub, H., and Gim, D.-W., "Gravitational Perturbations, Nonlinearity and Circular Orbit Assumption Effects on Formation Flying Control Strategies," American Astronautical Society, AAS Paper 00-012, Feb. 2000.

[9]Mitchell, J. W., and Richardson, D. L., "Maintaining Periodic Trajectories with the First-Order Nonlinear Hill's Equations," American Astronautical Society, AAS Paper 01-473, July–Aug. 2001.

[10]Broucke, R. A., "A Solution to the Elliptic Rendezvous Problem with Time as the Independent Variable," American Astronautical Society, AAS Paper 02-144, Jan. 2002.

[11]Yamanaka, K., and Ankersen, F., "New State Transition Matrix for Relative Motion on an Arbitrary Elliptical Orbit," *Journal of Guidance, Control, and Dynamics*, Vol. 25, No. 1, 2002, pp. 60–67.

[12]Prussing, J. E., and Conway, B. A., Orbital Mechanics, Oxford Univ. Press, Oxford, 1993, p. 149.